A Low-cost, Smartphone-only Pulse Transit Time Measurement System Using Cardio-mechanical Signals and Optical Sensors*

Chenxi Yang, *Student Member,* Yudi Dong, *Student Member*, Yingying Chen, *Senior Member*
Negar Tavassolian, *Member, IEEE*

Abstract— **This paper presents a smartphone-only solution for measuring pulse transit time (PTT). An application based on an Android smartphone is developed to collect seismocardiogram (SCG), gyrocardiogram (GCG), and photoplethysmography (PPG) recordings. The system does not need any other external system for measurements, so the total cost and system complexity are minimized. PTT metrics are calculated as the time difference between the aortic valve opening points in the SCG or GCG signals recorded by the accelerometer or gyroscope of a smartphone respectively, and the fiducial points in the PPG signal recorded by a modified optical sensor connected to the audio input. A digital signal processing (DSP) system is developed in a post-processing environment and experimentally validated on ten healthy subjects at rest. Our results indicate that a smartphone-only PTT measurement system is feasible and comparable with stand-alone sensor node systems.**

I. INTRODUCTION

Blood pressure (BP) is the pressure of blood circulation in blood vessels [1]. Blood pressure values variations represent the functioning of the cardiovascular system and could yield early indicators of cardiovascular diseases such as hypertension, hypertensive heart disease, atrial fibrillation, and stroke [1]. The self-management and monitoring of BP is therefore an essential part of the prevention and treatment of BP-related diseases, either providing early detection of abnormalities in BP values or tracking the effectiveness of the routine medication. Oscillometry, volume clamp, and auscultation are the most widely used non-invasive BP monitoring methods that are employed in both clinical and home applications. However, most of these cuff-based methods cannot provide continuous monitoring of BP, which hinders them from detecting immediate BP variations which are the early symptom of many types of cardiovascular diseases (CVDs) [2]. Moreover, the natural need for a bulky cuff brings extra inconvenience to subjects who need to take long-term measurements during daily activities.

Pulse transit time (PTT) is defined as the time taken by the pulse wave to travel in the blood vessels. An arterial PTT describes the time elapse of the BP pulse to travel from a proximal arterial site to the arrival point at a distal arterial location [2]. The velocity of this traveling pulse has been reported to be correlated with blood pressure [2], [3]. A rising BP will shorten the PTT proportionally, and the variation can be monitored in a beat-by-beat manner. Therefore, the

measurement of PTT has been suggested as a non-invasive and continuous method for arterial BP estimation without the need for cuffs.

In most literature, PTT is approximated by the pulse arrival time (PAT), which is defined as the time difference from the R-peak of the electrocardiogram (ECG) signal to the peak or foot of a distal photoplethysmography (PPG) recording [2], [3]. However, the effectiveness of using PAT to estimate BP has been questioned in the literature, as the pre-ejection period in PAT can confound the results [2], [4].

Cardio-mechanical signals, namely seismo-cardiography (SCG) and gyro-cardiography (GCG), are wearable sensing modalities that have been enthusiastically researched in recent years [5]-[7]. The seismo- and gyro-cardiogram signals can be measured by placing accelerometers and gyroscopes, respectively, on the sternum of subjects. The fiducial points in SCG and GCG represent the timing of the aortic valve opening (AO) event [7], which can provide accurate proximal timing information without the interference of the pre-ejection period. Several recent studies have verified that PTT can be effectively acquired by stand-alone wearable hardware systems based on cardio-mechanical signals and PPG recordings [8]-[10].

From the perspective of implementing a future out-of-clinic BP monitoring system based on PTT measurement devices [8]-[10], a mobile device with the capabilities of short- and long-range wireless communication and data analysis will be required as the intermediate node between the stand-alone device and healthcare providers. As shown in Fig. 1 (a), a smartphone, for instance, could be the node that communicates with both the measurement device and the hospital. It can also work as an interface where the user receives timely alarms and BP management suggestions. However, such a setup has several disadvantages. The first is that the cost of a stand-alone device would be high due to the need for micro-processors and communication modules. The second drawback is that the battery life of stand-alone sensing systems is generally limited by their size (due to form factor) and power consumption (due to wireless data streaming), limiting the capability of the
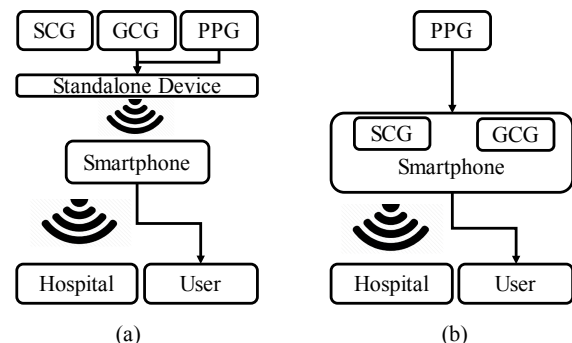

Fig. 1. (a) The BP monitor system with stand-alone devices. (b) The BP monitor system with proposed smartphone-only solution.

system for long-term monitoring. Modern smartphones have shown sufficient capability in providing cardio-mechanical measurements using their internal inertial measurement unit (IMU) [11]-[13]. In our preliminary work in [13], we investigated the feasibility of acquiring cardio-mechanical signals that are reliable in temporal accuracy from the IMUs of an Android smartphone. Experimental data indicated that the calculations of PTT based on seismo- and gyro-cardiogram signals from the smartphone and the PPG signal from a stand-alone reference sensor were comparable with fully stand-alone PTT measurement results.

In this paper, we push forward the work in [13] by using a modified optical sensor that connects to the smartphone via the audio input jack for PPG signal recordings. As illustrated in Fig. 1 (b), the proposed smartphone-only solution has a simpler system design and a much lower cost, as no external devices are needed in this setup. A smartphone application along with a digital signal processing (DSP) system that handles the acquisition, reconstruction, and analysis of all the signals is developed and experimentally tested. The accuracy of the results is confirmed through comparison with the stand-alone device measurements.

II. METHOD

A. The Hardware System

The hardware system setup is shown in the left side of Fig. 2. It consists of the smartphone-only PTT measurement system and a stand-alone reference device. The details are as follow.

1) The smartphone-only setup

A Motorola X (Android Version: 5.0) smartphone was used in this study. As illustrated in Fig. 2, the smartphone is placed on the chest wall of the subject at the center of the sternum along the third rib with an elastic belt (removed in Fig. 2 to show the overlay of two devices). The smartphone is horizontally placed so that the z-axis of the internal accelerometer represents the dorso-ventral axis of the subject. Moreover, the pitch and roll axes of the internal gyroscope agree with the x- and y-axis of the reference sensor node respectively, which is presented by the axis system in Fig. 2. A PPG sensor (SON1303+3130, SOON Electronic Co., Inc.) is attached to the index finger of the subject, marked by the orange circle at the left side in Fig. 2.

The voltage level of the PPG analog front-end is 0-3.3 V, which is much higher than the input range of the audio analog-to-digital (ADC) converter in smartphones. Also, the
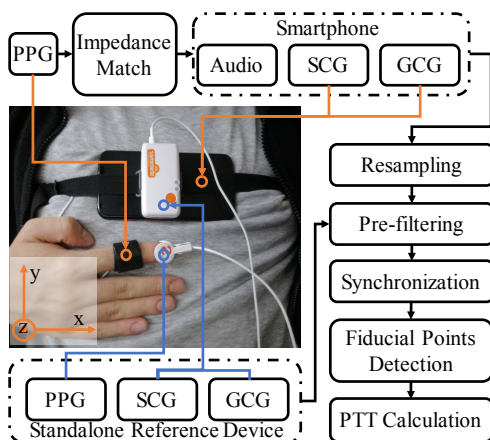
smartphone has an impedance detection circuit in compliance with the Android standard which only accepts inputs with a certain impedance range. Moreover, a DC voltage bias from 1.2-1.5 V is applied to the audio input of the smartphone to drive the microphones, which will interfere with the analog output of the PPG sensor if not isolated. To address these issues, we built a circuit consisting of an operational amplifier and an impedance network to connect between the PPG output and the audio input of the smartphone. Fig. 3 illustrates the prototype circuit. The active components of this circuit are powered by the universal serial bus (USB) port of the smartphone, which provides DC voltage using the function of USB *on-the-go* (OTG). The circuit translates the impedance to 2000 Ohms with a peak-to-peak voltage of 200 mV. The analog signal is then transmitted via a standard tip-ring-sleeve (TRS) audio cable to a tip-ring-ring-sleeve (TRRS) adapter which plugs into the smartphone audio jack.

2) The reference sensor node setup

A commercial wearable sensor node (Shimmer 3 from Shimmer Sensing, pointed at by the blue circle on the top in Fig. 2) is attached on top of the smartphone using a separate chest strap (shown in Fig. 2). A three-axis micro-electro-mechanical system (MEMS) accelerometer (Kionix KXRB5-2042, Kionix, Inc.) measures the SCG signal, and a three-axis MEMS gyroscope (Invensense MPU9150, Invensense, Inc.) records the GCG graph. In addition, a finger-tip PPG sensor is connected to the same index finger of the subject as indicated by the blue circle at the bottom of Fig. 2 for comparison with the cell-phone PPG signal. The axis system of the reference sensor defines the z-axis as the dorso-ventral direction of the body. As shown in Fig. 2, the y-axis is along the head-to-foot direction while the x-axis is along the shoulder-to-shoulder direction. The accelerometer and gyroscope ranges are ±2 g and ±250 degrees-per-second (DPS) respectively, and all the sensors are sampled at a rate of 256 Hz. Data are transmitted via Bluetooth to a computer for processing.

B. The Software System

1) The smartphone application

The smartphone application includes two main activities in parallel. The first activity of the application is the recording of seismo- and gyro-cardiogram signals by accessing the *SensorEvent* with *SensorEventListener*, which is introduced in detail in [13]. During each data recording cycle, the *timestamp* and *values* of the *SensorEvent*s are recorded and stored in a comma-separated value (CSV) file. The nominal refresh rate used in the study is 180 Hz. As mentioned in Section II.A.1, the *gyro_roll* data from the *values* corresponds to the y-axis,
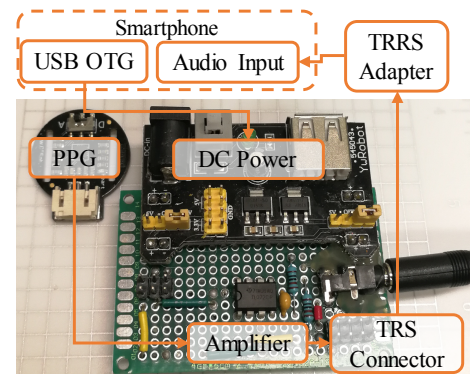

Fig. 2. Illustration of the proposed hardware setup and the diagram of the DSP infrastructure.

Fig. 3. Modified PPG prototype circuit with audio-input compatibility for smartphones.

3806

and the *z-axis acceleration* agrees with the z-axis. The second activity is an audio-recording activity that utilizes the *MediaRecorder*. The sampling rate is set to 44,100 Hz with a *minimum* buffer size to control the input delay. Also, a round-trip delay test is used to calculate and compensate the audio ADC delay using the method described in [8]. The starting *timestamp* of the audio recording is also recorded to synchronize the PPG signal with the cardio-mechanical recordings. The smartphone is configured in the *developer* mode with the highest priority for the proposed application.

2) The DSP programs

The right side of Fig. 2 describes the structure of the DSP programs. Only the *z*-axis seismo-cardiogram signal is selected in this study for both the smartphone and the reference sensor node. This signal is commonly referred to as the single-axis SCG waveform and contains the major portion of heart-induced linear accelerations of the chest wall [5]. The gyrocardiogram signal is selected as the rotational information along the *y*-axis, i.e., the gyro_roll axis of the smartphone. This axis has been reported to have the highest quality among the three axes [6], [7].

The PPG from the smartphone is uniformly resampled to 128 Hz for the consistency of further processing steps. The seismo- and gyro-cardiogram recordings are non-uniformly resampled to 128 Hz based on the recorded *timestamp* using a spline interpolation. Our previous work has indicated that the non-uniform sampling is beneficial to the calculation of PTT due to the unstable sampling frequency of the internal IMU [13].

Both the resampled recordings from the smartphone and the reference recordings from the stand-alone device are then pre-filtered to focus on the informative bandwidths and remove baseline variations. The SCG and GCG signals are filtered with a zero-phase infinite impulse response (IIR) bandpass filter with a pass band from 0.8 Hz to 25 Hz. The PPG signals are filtered from 0.8 Hz to 60 Hz with the same type of IIR filter. Moreover, the audio and IMU recordings from the smartphone are smoothened with a 10th order moving average filter.

After pre-filtering, all the signals are synchronized to the same timeframe in two steps. The first step is the synchronization between the cardio-mechanical signals and PPG recordings from the smartphone. The time offset between these two types of recordings are expressed in the following equation.

$$t = |ts_{audio} - ts_{IMU}| + delay_{ADC} \qquad (1).$$

In equation (1), *ts* indices represent the starting timestamps of audio and IMU recordings respectively, and the *delay_{ADC}* is the round-trip audio delay. In our setup, this delay is tested as 47 milliseconds (ms). The time-offset *t* is then used to adjust the timestamps to match each other. The next step of synchronization is between the smartphone recordings and reference recordings. A tapping method is used in this step. At the beginning of the measurement, a firm tapping is applied to the top of the reference device in the *z*-axis direction. A maximum searching algorithm is then used to find the indices of the tapping signal in the IMU recordings from both smartphone and the reference device. Then the difference between these two indices is used to adjust the timestamps between smartphone recordings and reference recordings.

Following the synchronization step, the fiducial points are extracted from all the recordings. The distal timing indicator is selected to be the systolic maximum in the PPG recordings, which is detected by a local maximum searching algorithm with the minimum threshold as 60% of the maximum amplitude and a minimum distance of 250 ms between adjacent peaks. The indices that point to these systolic-maximum points are defined as $I_{PPG}(i)$. The proximal timing indicators are then located with the equations below.

$$IM_{SCG}(i) = \min_{index}{}_{t=I_{PPG}(i)}^{I_{PPG}(i+1)}(SCG) \qquad (2).$$

$$AO_{SCG}(i) = \max_{index}{}_{t=IM(i)}^{IM(i)+150ms}(SCG) \qquad (3).$$

$$AO_{GCG}(i) = \max_{index}{}_{t=I_{PPG}(i)}^{I_{PPG}(i+1)}(GCG) \qquad (4).$$

In these equations, *i* ranges from 1 to *n-1*, where *n* represents the number of peaks. *IM* is the index of the local minimum point between every two PPG maximum points, which biophysically represents the isovolumic moment during each cardiac cycle. Then the first maxima after the *IM* indices in SCG are marked as the AO indices. The AO selection from GCG is relatively more straightforward with one single step of locating the maximum in each cardiac cycle.

Six different PTT values, defined as PTT_{1-6}, are then calculated as the time differences between proximal and distal indicators. PTT_{1-2} are calculated with purely smartphone recordings, from SCG and GCG points to the PPG fiducial points respectively. PTT_{3-4} are the same calculations with purely reference recordings from SCG and GCG successively. PTT_{5-6} are defined as described in [13], in which PTT is calculated from smartphone SCG and GCG signals to the reference PPG signal. PTT_{1-2} represent the results of the proposed new work, which will be compared with reference values (PTT_{3-4}) and the results of the previous method of [13] (PTT_{5-6}). A valid PTT is defined as a measurement which is within 50% error range compared to reference values. A PTT with an error above this value is considered a miss-detection and will be excluded from further PTT analyses. The error value of 50% is also considered for calculating the detection rate of PTT cycles.

III. Experimental Setup and Results

A. Experimental Setup

Ten healthy adult subjects (average age: 25, average height: 65 inches, average weight: 130 lbs) participated in this study. The subjects were required to lie flat on a bed for 5 minutes during each experiment. They breathed naturally without intensively controlling their breathing depths. All human experiments were approved by the Committee for the Protection of Human Subjects at Stevens Institute of Technology under protocol number 2017-008 (N).

B. Experimental Results

1) PTT measurement results

Table I summarizes the PTT measurement results from PTT_{1-6}. PTT_2 reports the PTT measurement from GCG to PPG using smartphone sensors. Compared to PTT_4 from the reference device which is considered as the ground truth in this study, the largest absolute error between PTT_2 and PTT_4 in average value is 7.7 ms (Subject 5). While using the previous method, the largest absolute error between PTT_6 and PTT_4 is 8.9 ms (subject 6) in average. Moreover, the root mean square error (RMSE) from all subjects has a value of 3.93 for PTT_2, which is smaller than the value of 4.68 for PTT_6. This result suggests that the smartphone-only solution improves the PTT measurement precision from GCG compared to the previous method in [13]. On the other hand, with PTT measurements

3807

Subject	PTT from smartphone		PTT from reference device		PTT from previous method in [13]	
	PTT$_1$ (SCG)	PTT$_2$ (GCG)	PTT$_3$ (SCG)	PTT$_4$ (GCG)	PTT$_5$ (SCG)	PTT$_6$ (GCG)
1	189.8 ± 14.1	185.6 ± 24.8	187.2 ± 17.6	186.4 ± 25.0	191.1 ± 22.5	185.2 ± 31.2
2	184.3 ± 8.8	188 ± 10.9	185.8 ± 5.7	187.8 ± 15.2	188.4±10.1	187.5 ± 15.9
3	192.7 ± 18.7	190.9 ± 21.0	189.8 ± 31.6	189.6 ± 51.2	186.9±35.5	189.2 ± 30.4
4	147.8 ± 22.1	142.7 ± 18.8	145 ± 11.7	145.9 ± 20.0	152.5±24.6	153.2 ± 21.2
5	195.3 ± 8.38	196.2 ± 9.7	190.5 ± 5.6	188.5 ± 14.9	198.3±12.2	193.0 ± 12.5
6	116.2 ± 44.3	120.4 ± 45.3	119.3 ± 42.5	115.4 ± 30.1	125.2±42.5	124.3 ± 37.1
7	155.1 ± 30.6	149.7 ± 29.1	144.2 ± 21.2	145.1 ± 33.4	150.6±23.4	149.7 ± 28.6
8	154.8 ± 11.8	163.1 ± 10.4	159.8 ± 8.3	157.8 ± 12.3	166.7±14.2	164.3 ±16.8
9	204.8 ± 12.5	202.2 ± 23.5	202.9 ± 7.8	204.6 ± 36.9	199.1±25.0	204.4 ± 26.6
10	155.7 ± 52.8	156.6 ± 31.4	150.8 ± 34.1	153.3 ± 39.7	154.9±47.8	154.3 ± 26.09

based on SCG, the maximum absolute error between PTT$_1$ and PTT$_3$ is 10.9 ms (subject 7), which is larger than the maximum error of 7.8 ms between PTT$_5$ and PTT$_3$ (subject 5). However, the RMSE value for the smartphone-only solution is still smaller than the RMSE value for the previous method (4.77 versus 5.46). The Bland-Altman plot from one representative subject comparing PTT$_2$ and PTT$_4$ is illustrated in Fig. 4. It is shown that most of the measurements are within the 95% agreement limit borders.

In conclusion, PTT measurements based on the smartphone-only solution outperform our previous method due to the integration of all the signals in the same device, which eliminates potential errors occurring during inter-device synchronization. Moreover, the results from GCG-based PTT slightly outperform the results from SCG-based PTT which is consistent with our previous method results.

2) Beat-to-beat detection of PTT

The detection rate is defined as the number of valid PTT estimations from smartphone-only method over the number of estimations from the reference device. The overall detection rates of PTT cycles from 10 subjects are 93.63% (1176/1256) from GCG and 92.75% (1165/1256) from SCG. Compared to our previous method with detection rates of 93.12% and 91.86% respectively, no significant improvement has been gained from using the smartphone-only solution. This result was expected as miss-detection is mostly caused by the lower quality of the SCG and GCG signals from the IMU in smartphones compared to the IMU in stand-alone devices.

IV. DISCUSSION AND CONCLUSIONS

This paper introduces a novel smartphone-only PTT measurement system based on an Android application which
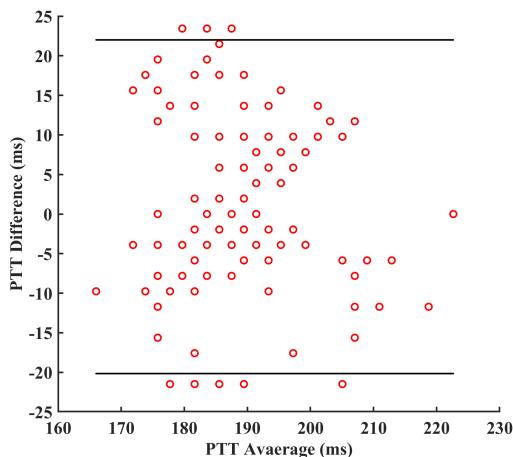

Fig. 4. Bland-Altman plot of PTT results between smartphone-only solution and reference device from one representative measurement (black horizontal lines represent the 95% agreement limit borders).

utilizes the internal inertial sensor of a smartphone and a customized PPG sensor that connects to the audio input of the phone. Experimental results validate the feasibility of the system to estimate PTT with a comparable performance to a dedicated embedded system.

Our future work includes incorporating an energy harvester at the audio output of the smartphone like the one in [14] to further simplify the system complexity. Moreover, the quality of seismo- and gyro-cardiogram recordings could be potentially improved by utilizing all the axes of SCG and GCG recordings.

REFERENCES

[1] D. Mozaffarian, *et al.*, "Executive Summary: Heart Disease and Stroke Statistics-2016 Update: a Report from the American Heart Association," *Circulation*, vol. 133, no. 4, p. 447, 2016.

[2] R. Mukkamala, *et al.*, "Toward Ubiquitous Blood Pressure Monitoring via Pulse Transit Time: Theory and Practice," *IEEE Trans. on Biomed. Eng.*, vol. 62, no. 8, pp. 1879-1901, Aug. 2015.

[3] H. Gesche, *et al.*, "Continuous Blood Pressure Measurement by Using the Pulse Transit Time: Comparison to a Cuff-Based Method," *Eur. J. Appl. Physiol.*, vol. 112, pp. 309–315, 2012.

[4] G. Zhang, *et al.*, "Pulse Arrival Time is not an Adequate Surrogate for Pulse Transit Time as a Marker of Blood Pressure," *J. Appl. Physiol.*, vol. 111, pp. 1681–1686, 2011.

[5] Paukkunen, Mikko. "Seismocardiography: Practical Implementation And Feasibility." PhD Dissertation, Dep. of Elec. Eng. and Auto., Aalto University, 2014.

[6] Tadi Mojtaba Jafari, *et al.*, "Gyrocardiography: A New Non-invasive Monitoring Method for the Assessment of Cardiac Mechanics and the Estimation of Hemodynamic Variables." *Sci. Reports*, vol.7, 2017.

[7] C. Yang, N. Tavassolian, "Combined Seismo- and Gyro-cardiography: A More Comprehensive Evaluation of Heart-Induced Chest Vibrations," *IEEE J. of Biomed. and Health Info.*, vol. PP, no. 99, pp. 1-1.

[8] C. Yang and N. Tavassolian, "Pulse transit time measurement using seismocardiogram and in-ear acoustic sensor," *IEEE Biom. Circuits and Sys. Conf. (BioCAS)*, pp. 188-191, 2016.

[9] M. Di Rienzo, *et al.*, "A new technological platform for the multisite assessment of 3D seismocardiogram and pulse transit time in cardiac patients," *2016 Computing in Cardio. Conf. (CinC), Vancouver, BC*, 2016, pp. 781-784.

[10] A. K. Verma, *et al.* "Pulse Transit Time Derivation using Xiphoidal and Carotid Seismocardiograms." *2017 Design of Med. Devices Conf. American Soc. of Mech. Engineers*, pp. V001T01A010-V001T01A010, 2017.

[11] O. Lahdenoja, *et al.*, "A Smartphone-Only Solution For Detecting Indications Of Acute Myocardial Infarction," *2017 IEEE Int. Conf. on Biomed. & Health Info. (BHI), Orlando, FL, 2017*, pp. 197-200.

[12] O. Lahdenoja, *et al.*, "Atrial Fibrillation Detection via Accelerometer and Gyroscope of a Smartphone," *in IEEE J. of Biomed. and Health Info.*, vol.PP, no.99, pp.1-1, 2017.

[13] C. Yang, N. Tavassolian, "A feasibility study on a low-cost, smartphone-based solution of pulse transit time measurement using cardio-mechanical signals," *2017 IEEE Health. Inno. and Point of Care Tech. (HI-POCT)*, pp. 93-96.

[14] Y.S. Kuo, *et al.*, "Hijacking power and bandwidth from the mobile phone's audio interface." *Proceedings of the First ACM Symposium on Computing for Development*, pp. 24, 2010.